MIT Open Access Articles

A decomposition-based uncertainty quantification approach for environmental impacts of aviation technology and operation

Massachusetts Institute of Technology

A Decomposition-Based Uncertainty Quantification Approach for Environmental Impacts of Aviation Technology and Operation

Sergio Amaral, Douglas Allaire, Elena de la Rosa Blanco, Karen Willcox

Abstract. As a measure to manage the climate impact of aviation, significant enhancements to aviation technologies and operations are necessary. When assessing these enhancements and their respective impacts on the climate, it is important that we also quantify the associated uncertainties—this is important to support an effective decision and policy making process. However, such quantification of uncertainty is challenging, especially in a complex system that comprises multiple interacting components. The uncertainty quantification task can quickly become computationally intractable and cumbersome for one individual or group to manage. Recognizing the challenge of quantifying uncertainty in multicomponent systems, we utilize a divide-and-conquer approach, inspired by the decomposition-based approaches used in multidisciplinary analysis and optimization. Specifically, we perform uncertainty analysis and global sensitivity analysis of our multicomponent aviation system in a decomposition-based manner. In this work we demonstrate how to handle a high-dimensional multicomponent interface using sensitivity-based dimension reduction and a novel importance sampling method. Our results demonstrate that the decomposition-based uncertainty quantification approach can effectively quantify the uncertainty of a feed-forward multicomponent system for which the component models are housed in different locations and owned by different groups.

Key words.

1. Introduction.

The aviation sector is projected to be one of the fastest growing contributors to anthropogenic greenhouse gas emissions [19]. If left unconstrained, the emissions from aircraft in 2050 are projected to be quadruple the emissions from aircraft in 2006 [1]. Many groups are using simulation-based tools to study technologies, designs, and policies that address this challenge. In conducting such studies, it is critical to quantify the effects of uncertainties and to account for their impacts in decision-making. Yet, uncertainty quantification for such a complex multicomponent system—with multiple components ranging from individual aircraft technologies to fleet-wide operations—is a significant challenge. This paper demonstrates how a decomposition-based approach can manage the complexity to make uncertainty quantification tractable for a large-scale feed-forward problem in environmental impacts of aviation technology and operation. Our problem is large scale in several regards: the dimension of the uncertain parameter space is 12; there are 100 variables describing the coupling between the two components; and a single analysis (forward simulation) of the system takes approximately 3 minutes on a desktop computer. To manage the high-dimensional multicomponent interface, we apply a combination of dimension reduction to identify the important coupling variables and importance sampling to transform the information across the interface in an efficient and dependable manner.

As a measure to manage the climate impact of aviation, the Committee for Environmental Protection (CAEP) under the International Civil Aviation Organization (ICAO) and with support from the Federal Aviation Administration (FAA), adopted a 2% annual efficiency improvement goal for aviation through 2050 [2]. To satisfy this fast paced fleet-wide improvement requires significant enhancements to aviation technology, sustainable fuels with low CO_2 emissions, and efficient operational procedures [26]. To meet these demanding requirements,

CAEP assembled a panel of independent experts with varying backgrounds to establish long-term technology goals for aviation fuel consumption [14]. Within their study they investigated future aviation technology scenarios, which represented varying regulatory pressure to reduce fuel consumption. The future aircraft technology scenarios were then applied in analysis tools as "technology packages" to assess the technology improvement on aircraft fuel consumption. However, these technological enhancements are inherently uncertain and thus their respective impacts on the environment are also uncertain.

Through a rigorous characterization and management of uncertainty, one can provide quantitative estimates of uncertainty necessary to calculate relevant statistics and event probabilities. However, to estimate relevant statistics and event probabilities requires an uncertainty quantification of the entire system. Uncertainty quantification is a broad field encompassing a number of different aspects [30]; this work focuses on uncertainty analysis and global sensitivity analysis. The objective of an uncertainty analysis, also known as forward propagation of uncertainties, is to quantify the distribution of the output of interest, given distributions on the uncertain input variables. The objective of a global sensitivity analysis is to apportion variability in the output quantity of interest according to contributions from the uncertain input variables and their interactions.

Quantifying uncertainty of an entire system may be cumbersome due to factors that result in inadequate integration of engineering disciplines, subsystems, and parts, which we refer to collectively here as components. Such factors include components managed by different groups, component design tools or groups housed in different locations, component analyses that run on different platforms, components with significant differences in analysis run times, lack of shared expertise amongst groups, and the sheer number of components comprising the system. These challenges are only heightened by the fact that globalization has spread the design and analysis of the complex systems throughout the world. Recognizing the challenge of quantifying uncertainty in multicomponent systems, we establish a divide-and-conquer approach, inspired by the decomposition-based approaches used in multidisciplinary analysis and optimization [10, 18, 31, 16].

Previous works have tackled these challenges through the use of surrogate modeling and/or a simplified representation of the uncertainty. Using surrogates in place of the higher fidelity components in the system provides computational gains and also accommodates the task of integrating components [21]. Using a simplified uncertainty representation (e.g., using mean and variance in place of full distributional information) bypasses the need to propagate the full nonparametric uncertainty from one component to another. Such simplifications are commonly used in uncertainty-based multidisciplinary design optimization methods as a way to avoid a system-level uncertainty analysis (see e.g., [32] for a review of these methods and their engineering applications). Other methods have exploited the structure of the multicomponent system to manage the complexity of the system uncertainty analysis where the system contains a feedback loop [5, 6, 7, 13, 29, 11]. Additionally, previous works have tackled decomposition-based global sensitivity analysis within the application of feed-forward systems. A top-down (i.e., assuming that all system variables are independent) sensitivity analysis strategy was developed to determine critical components in the system and used a simplified formulation to evaluate the main sensitivity indices [33, 20]. Limitations in these existing approaches include the introduction of approximations of the components comprising the system, parametric ap-

proximations of the uncertainty, a need to repeatedly evaluate the system in its entirety, and a need to apply correlation between system variables to account for dependency structure. Instead, we approach the problem using a decomposition-based vision of the multicomponent uncertainty quantification task—performing uncertainty quantification on the respective components individually, and assembling the component-level uncertainty quantifications to quantify the system uncertainty.

In Section 2, we introduce the multicomponent aviation system of interest and describe its constituent components: the aircraft technology component and aviation environmental impacts component. In Section 3, we present the coupling between the aircraft technology component and the aviation environmental impacts component. We discuss the challenges that arise from this component-to-component coupling and our proposed solution for overcoming said challenges. Our decomposition-based uncertainty quantification approach is introduced in Section 4 along with the uncertainty quantification results. Our results are compared to the standard Monte Carlo simulation of the entire system. Lastly, our conclusion and future work are provided in Section 5.

2. Systems modeling of aviation environmental impacts. The multicomponent system of interest consists of a conceptual-level aircraft design component, the Transport Aircraft System OPTimization (TASOpt) [15], and an aviation environmental impacts component, the Aviation Environment Design Tool (AEDT) version 2a [25]. This multicomponent system is depicted in its entirety in Figure 1.

2.1. Transport Aircraft System Optimization (TASOpt). The TASOpt component is an aircraft performance tool that allows users to evaluate and size future aircraft with potentially novel airframe, aerodynamic, engine, or operation variables using low-order physical models implementing fundamental structural, aerodynamic, and thermodynamic theory. TASOpt uses historical-based correlations only when necessary, in particular only for some of the secondary structure and aircraft equipment. The TASOpt component takes as input aircraft technology and operational variables and can either optimize an aircraft over a specified set of constraints or resize an aircraft to meet a desired mission requirement. The aircraft configuration selected for this study is the Boeing 737-800W shown in Figure 2. This aircraft operates in the short-to-medium range while seating approximately 180 passengers.

Table 1 contains the 27 uncertain TASOpt random input variables selected for this study and their respective distributions. These input variables represent the technological and operational variables of an aircraft that are considered to be uncertain in the design phase. The uncertainty associated with the technology input variables captures our lack of knowledge due to material properties and measurement capabilities. The uncertainty associated with the operational input variables captures the designer lack of knowledge in the design phase of an aircraft. We start by defining a baseline aircraft. The baseline aircraft configuration used for this study was created using TASOpt's optimization capabilities to best represent the Boeing 737-800W aircraft configuration (defined in Figure 1's "Boeing 737-800 Template Input File"). We then generate a realization of the random variables associated with each of the 27 input variables in Table 1. This defines a "sampled aircraft." Next TASOpt resizes this sampled aircraft in order to ensure that it is a feasible aircraft.
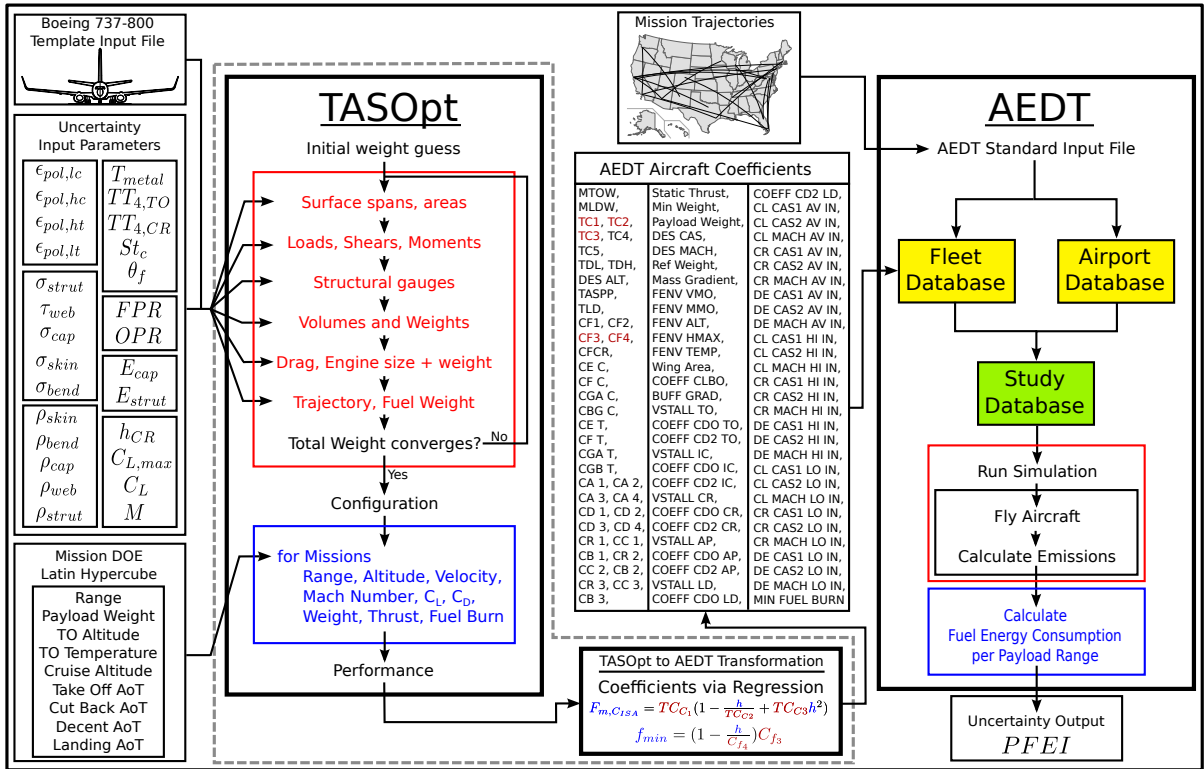
Boeing 737-800
Template Input File

Mission Trajectories

TASOpt

Initial weight guess

AEDT Aircraft Coefficients

AEDT

AEDT Standard Input File

Uncertainty
Input Parameters

$\epsilon_{pol,lc}$ T_{metal}
$\epsilon_{pol,hc}$ $TT_{4,TO}$
$\epsilon_{pol,ht}$ $TT_{4,CR}$
$\epsilon_{pol,lt}$ St_c
           θ_f

σ_{strut}
τ_{web} FPR
σ_{cap} OPR
σ_{skin} E_{cap}
σ_{bend} E_{strut}

ρ_{skin} h_{CR}
ρ_{bend} $C_{L,max}$
ρ_{cap} C_L
ρ_{web} M
ρ_{strut}

Surface spans, areas

Loads, Shears, Moments

Structural gauges

Volumes and Weights

Drag, Engine size + weight

Trajectory, Fuel Weight

Total Weight converges? No

Yes

Configuration

MTOW,
MLDW,
TC1, TC2,
TC3, TC4,
TC5,
TDL, TDH,
DES ALT,
TASPP,
TLD,
CF1, CF2,
CF3, CF4,
CFCR,
CE C,
CF C,
CGA C,
CBG C,
CE T,
CF T,
CGA T,
CGB T,
CA 1, CA 2,
CA 3, CA 4,
CD 1, CD 2,
CD 3, CD 4,
CR 1, CC 1,
CB 1, CR 2,
CC 2, CB 2,
CR 3, CC 3,
CB 3,

Static Thrust,
Min Weight,
Payload Weight,
DES CAS,
DES MACH,
Ref Weight,
Mass Gradient,
FENV VMO,
FENV MMO,
FENV ALT,
FENV HMAX,
FENV TEMP,
Wing Area,
COEFF CLBO,
BUFF GRAD,
VSTALL TO,
COEFF CD0 TO,
COEFF CD2 TO,
VSTALL IC,
COEFF CD0 IC,
COEFF CD2 IC,
VSTALL CR,
COEFF CD0 CR,
COEFF CD2 CR,
VSTALL AP,
COEFF CD0 AP,
COEFF CD2 AP,
VSTALL LD,
COEFF CD0 LD,

COEFF CD2 LD,
CL CAS1 AV IN,
CL CAS2 AV IN,
CL MACH AV IN,
CR CAS1 AV IN,
CR CAS2 AV IN,
CR MACH AV IN,
DE CAS1 AV IN,
DE CAS2 AV IN,
DE MACH AV IN,
CL CAS1 HI IN,
CL CAS2 HI IN,
CL MACH HI IN,
CR CAS1 HI IN,
CR CAS2 HI IN,
CR MACH HI IN,
DE CAS1 HI IN,
DE CAS2 HI IN,
DE MACH HI IN,
CL CAS1 LO IN,
CL CAS2 LO IN,
CL MACH LO IN,
CR CAS1 LO IN,
CR CAS2 LO IN,
CR MACH LO IN,
DE CAS1 LO IN,
DE CAS2 LO IN,
DE MACH LO IN,
MIN FUEL BURN

Fleet
Database

Airport
Database

Study
Database

Run Simulation

Fly Aircraft

Calculate Emissions

Calculate
Fuel Energy Consumption
per Payload Range

for Missions
Range, Altitude, Velocity,
Mach Number, C_L, C_D,
Weight, Thrust, Fuel Burn

Performance

Mission DOE
Latin Hypercube

Range
Payload Weight
TO Altitude
TO Temperature
Cruise Altitude
Take Off AoT
Cut Back AoT
Decent AoT
Landing AoT

TASOpt to AEDT Transformation
Coefficients via Regression
$$F_{m,C_{ISA}} = TC_{C_1}(1 - \frac{h}{TC_{c_2}} + TC_{C3}h^2)$$
$$f_{min} = (1 - \frac{h}{C_{f_4}})C_{f_3}$$

Uncertainty Output
$PFEI$

Figure 1. *System-level uncertainty quantification of the toolset consists of quantifying how uncertainty in aircraft technologies and operations impacts the uncertainty in the output of interest, here the aircraft's payload fuel energy intensity (PFEI).*
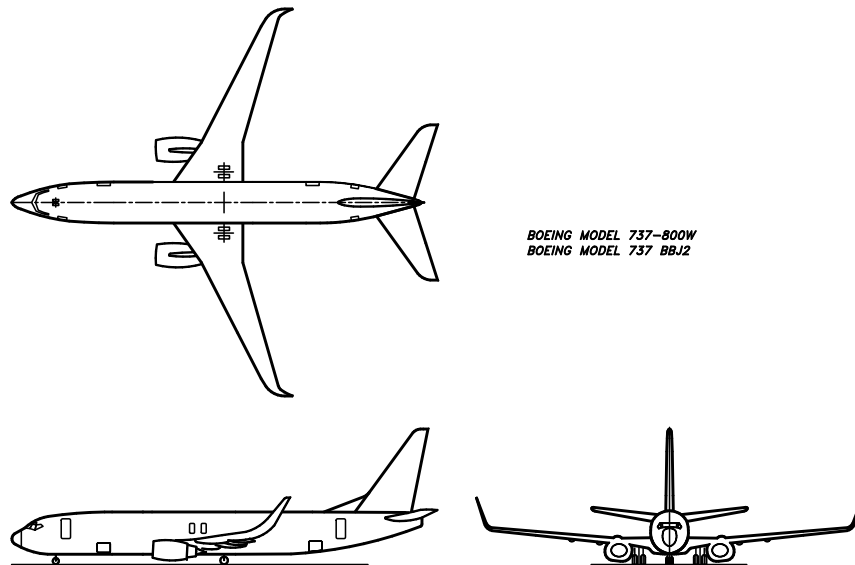
BOEING MODEL 737-800W
BOEING MODEL 737 BBJ2

Figure 2. *Boeing 737-800W airframe configuration. Schematic taken from [12].*

Table 1

TASOpt random input variables and their respective distributions.

Input	Description	Distribution	Units
$\epsilon_{pol,lc}$	low pressure compressor polytropic efficiency	$\mathcal{U}[0.936, 0.938]$	[-]
$\epsilon_{pol,hc}$	high pressure compressor polytropic efficiency	$\mathcal{U}[0.903, 0.904]$	[-]
$\epsilon_{pol,lt}$	low pressure Turbine polytropic efficiency	$\mathcal{U}[0.870, 0.872]$	[-]
$\epsilon_{pol,ht}$	high pressure Turbine polytropic efficiency	$\mathcal{U}[0.875, 0.877]$	[-]
σ_{strut}	max allowable strut stress	$\mathcal{U}[28500, 31500]$	[psi]
τ_{web}	max allowable wing spar web shear stress	$\mathcal{U}[19000, 21000]$	[psi]
σ_{cap}	max allowable wing spar cap stress	$\mathcal{U}[28500, 31500]$	[psi]
σ_{skin}	max allowable fuselage skin pressurization stress	$\mathcal{U}[14500, 15500]$	[psi]
σ_{bend}	max allowable fuselage shell bending stress	$\mathcal{U}[28500, 31500]$	[psi]
ρ_{strut}	strut material density	$\mathcal{U}[2672, 2726]$	[kg/m^3]
ρ_{web}	wing box web material density	$\mathcal{U}[2672, 2726]$	[kg/m^3]
ρ_{cap}	wing box cap material density	$\mathcal{U}[2672, 2726]$	[kg/m^3]
ρ_{skin}	fuselage pressure-skin density	$\mathcal{U}[2672, 2726]$	[kg/m^3]
ρ_{bend}	fuselage bending-material density	$\mathcal{U}[2672, 2726]$	[kg/m^3]
T_{metal}	turbine metal temperature	$\mathcal{U}[1172, 1272]$	[K]
$TT_{4,TO}$	turbine inlet total temperature for takeoff	$\mathcal{U}[1783, 1883]$	[K]
$TT_{4,CR}$	turbine inlet total temperature for cruise	$\mathcal{U}[1541, 1641]$	[K]
St_c	turbine area-weighted Stanton number	$\mathcal{U}[0.094, 0.096]$	[-]
Θ_f	film cooling efficiency	$\mathcal{U}[0.315, 0.325]$	[-]
FPR	fan pressure ratio	$\mathcal{U}[1.60, 1.62]$	[-]
OPR	operating pressure ratio	$\mathcal{U}[24.2, 28.2]$	[-]
E_{cap}	wing cap modulus of elasticity	$\mathcal{U}[9.5e6, 10.5e6]$	[psi]
E_{strut}	wing strut modulus of elasticity	$\mathcal{U}[9.5e6, 10.5e6]$	[psi]
h_{CR}	start-of-cruise altitude	$\mathcal{U}[34000, 36000]$	[ft]
$C_{L,max}$	maximum aircraft lift coefficient	$\mathcal{U}[2.2, 2.3]$	[-]
C_L	aircraft lift coefficient	$\mathcal{U}[0.576, 0.578]$	[-]
$Mach$	cruise flight Mach number	$\mathcal{U}[0.77, 0.79]$	[-]

The next step of the process quantifies the sampled aircraft's performance by flying 99 mission profiles, which are generated using a Latin hypercube design of experiments. The Latin hypercube design of experiments populates the 12 mission input variables contained in Table 2. Of the 100 mission profiles (baseline plus 99 additional missions) simulated in TASOpt, the first 50 are flown under international standard atmosphere (ISA) conditions while the remaining 50 are flown under non-ISA conditions. For any mission variable (e.g., Range) we generate 99 realizations from the uniform distribution (i.e., $\mathcal{U}(a,b)$) using the Latin hypercube sampling scheme and the parameters provided in Table 2. This process allows, for example, the *Range* to vary between 750 [nmi] and 3250 [nmi]. Lastly, the aircraft's configuration, operational procedure, and performance over multiple flight segments and atmospheric conditions are provided by the TASOpt component. This information is then transformed through a re-

gression process in order to construct a similar representative aircraft in the AEDT database. We shall discuss this multicomponent coupling procedure further in Section 3.

Input	Description	a	b	Units
$Range$	mission profile range	750	3250	[nmi]
W_{max}	average weight per passenger (180 passengers)	165	265	[lbs]
h_{TO}	altitude at takeoff	-4000	4000	[ft]
ΔT	temperature difference from ISA at takeoff	-12.5	12.5	[K]
h_{CR}	deviation of start-of-cruise altitude	-4000^*	4000^*	[ft]
$C_{L,max}$	deviation of maximum aircraft lift coefficient	-0.05^*	0.05^*	[-]
Θ_{TO}	angle of attack at takeoff	39	41	[deg]
Θ_{IC}	angle of attack at initial climb	2.8	3.2	[deg]
$\Theta_{DE,1}$	angle of attack at initial descent	-3.2	-2.8	[deg]
$\Theta_{DE,5}$	angle of attack at landing	-3.2	-2.8	[deg]
C_L	deviation of aircraft lift coefficient	-0.025^*	0.025^*	[-]
$Mach$	deviation of cruise flight Mach Number	-0.02^*	0.02^*	[-]

2.2. Aviation Environmental Design Tool (AEDT). The AEDT component is a suite of integrated aviation environmental impact tools. AEDT provides users with the ability to assess the interdependencies among aviation-produced fuel consumption, emissions, and noise. For cruise conditions the AEDT component implements the EUROCONTROL's Base of Aircraft Data (BADA) [23] which uses an energy-balance thrust model and thrust specific fuel consumption modeled as a function of airspeed. The BADA fuel consumption model has been shown to work well in cruise, with differences from airplane reported fuel consumption of about 5% [23]. For terminal conditions (e.g., departure/arrival flights until $10,000$ [ft] above ground level), the AEDT component implements a set of energy-balance equations to support a higher level of fidelity in fuel consumption modeling.

The AEDT component characterizes an aircraft using 100 input variables as depicted in Figure 1 as the "AEDT Aircraft Coefficients." A detailed description of the AEDT input variables are provided in the AEDT technical manual [17, 23]. These input variables characterize the aircraft's configuration and the operational procedure, and define the aircraft performance over multiple flight segments and atmospheric conditions. To initialize the AEDT component, we first generate a temporary Boeing 737-800W aircraft within the AEDT fleet database. Any TASOpt-generated aircraft then replaces the 100 aircraft input variables in the temporary Boeing 737-800 AEDT fleet database through the multicomponent coupling procedure described in the next section. The objective of the multicomponent coupling procedure is to ensure that an AEDT aircraft characterized through these 100 AEDT input variables is an adequate representation of the sampled TASOpt aircraft.

For each sampled aircraft we must quantify its respective environmental impacts. To do

so, we fly each sampled aircraft over a set of deterministic flight trajectories using the AEDT component. The flight trajectories for this study were selected from a 2006 representative day flight scenario database [22]. Using the representative day, the flights associated with the Boeing 737-700 aircraft are included as possible flight trajectories, since the Boeing 737-800W was not comprehensively represented in the 2006 representative day flight scenario. Twenty flight trajectories were selected; they are presented in Table 3 and illustrated in Figure 3. For computational purposes, these flight trajectories are approximated by a great circle path from the departure airport to the arrival airport. Each flight trajectory was generated by the TASOpt component using the baseline Boeing 737-800W aircraft configuration.

The output of interest, which we use to quantify an aircraft's environmental impacts, is the PFEI fuel consumption performance (i.e., fuel energy consumption per payload-range) and is defined as,

$$(2.1) \qquad PFEI = \frac{\sum_i W_{fuel,i} h_{fuel}}{\sum_i W_{pay,i} R_{total,i}},$$

where the summation is over number of missions, $W_{fuel,i}$ is the total fuel consumption of the ith mission, $R_{total,i}$ is the total range of the ith mission, $W_{pay,i}$ is the payload weight of the ith mission, and h_{fuel} is the specific heating value of kerosene.

Figure 3. *Illustrated here are the 20 representative flight trajectories flown by the Boeing 737-800W in the TASOpt-AEDT uncertainty quantification study.*

3. Multicomponent Coupling & Dimension Reduction. The objective of the multicomponent coupling procedure is to couple the tools and create a consistent representation of the system, i.e., to accurately represent the sampled TASOpt aircraft within the AEDT component. In this section we summarize the multicomponent coupling procedure and demonstrate how to transform the TASOpt outputs (i.e., aircraft configuration and performance) into AEDT inputs. We validate the multicomponent coupling by comparing the fuel consumption over similar scenarios (i.e., flight trajectories and operations) of a sampled TASOpt aircraft flown in TASOpt to that same aircraft imported into the AEDT component and flown in

Table 3
Presented here are the 20 representative flight trajectories (i.e., departure, arrival, and range) flown by the Boeing 737-800W in the TASOpt-AEDT uncertainty quantification study.

Depart Airport	Depart Runway	Arrival Airport	Arrival Runway	Range [nmi]
KDTW	04L	KPVD	21	535
KIAH	26L	KLAX	24L	1197
KLGA	22	KMEM	27	835
KDTW	04L	KSFO	28R	1801
KPDX	28R	KLAX	24L	725
KMIA	08L	KDEN	35R	1482
KPDX	28L	KABQ	08	964
KJFK	31R	KLGB	16L	2138
KIAD	01R	KORD	28	511
KPHX	26	KMSP	35	1106
KBWI	28	KFLL	09L	806
KPHX	26	KFLL	09L	1710
KMCO	35L	KDCA	01	662
KIAH	26L	KBOS	27	1387
KMCO	17R	KMKE	07R	928
KSJC	30R	KIAD	19L	2082
KSFO	28L	KPHX	25L	565
KDFW	35L	KSFO	28R	1270
KPHL	09R	KFLL	09L	864
KCLE	24L	KSFO	28R	1874

AEDT. Lastly, we reduce the dimensions of the multicomponent interface coupling by identifying which of the AEDT inputs have a significant impact on the systems output of interest uncertainty.

3.1. Multicomponent Coupling. The TASOpt component outputs the aircraft's configuration variables, which include the maximum takeoff weight, empty weight, maximum fuel weight, wing area, and maximum thrust. Additionally, the TASOpt component outputs the aircraft's performance for each mission, where each mission is composed of 15 individual flight segments (i.e., three takeoff, five climb, two cruise, and five descent segments). The TASOpt

generated aircraft performance data contains,

$$\begin{bmatrix} \text{Range} \\ \text{Altitude} \\ \text{True Airspeed} \\ \text{Mach Number} \\ \text{Lift Coefficient} \\ \text{Drag Coefficient} \\ \text{Aircraft Weight} \\ \text{Thrust} \\ \text{Fuel Burn Rate} \\ \text{Angle of Attack} \\ \text{Total Temperature at Engine Inlet} \\ \text{Total Pressure at Engine Inlet} \end{bmatrix}.$$

For demonstration purposes, we present an example of how to compute the AEDT thrust coefficients TC_{C_1}, TC_{C_2}, and TC_{C_3} in a flight's climbing segment and under ISA conditions. The AEDT aircraft thrust coefficients are related to the TASOpt outputs thrust, F, and altitude, h, by the following relation [17, 23],

$$(3.1) \qquad F = TC_{C_1} \cdot (1 - \frac{h}{TC_{C_2}} + TC_{C3} \cdot h^2).$$

To perform this transformation we use the TASOpt thrust and altitude performance data in the first 50 missions (i.e., under ISA conditions) and in the five climbing flight segments. With the TASOpt performance data collected, we perform a regression to obtain the AEDT coefficients using Equation 3.1. A similar procedure to the one explained here is performed for the remaining AEDT input variables. This multicomponent coupling procedure is depicted in Figure 1 as the "TASOpt to AEDT Transformation."

To validate our multicomponent coupling procedure we compare the total fuel consumption and relative error over three flight trajectories. The results from our validation study are provided in Table 4. The results indicate that we obtain a fair comparison between the two components. Of the three trajectories, Flight B had the highest relative error, however, this discrepancy can be attributed to how AEDT computes the aircraft's takeoff weight with respect to the flight trajectories range [17]. In Flight B, the AEDT takeoff weight was significantly higher than the TASOpt takeoff weight, which resulted in the increased total fuel consumption. The deviation in total fuel consumption in Flight A and Flight C are significantly lower than Flight B, since the AEDT aircraft takeoff weight was approximately equal to the TASOpt aircraft takeoff weight.

3.2. Dimension Reduction. The challenge with performing a decomposition-based uncertainty quantification of the system illustrated in Figure 1 lies in the high-dimensional multicomponent interface. The reason this is challenging is because our decomposition-based uncertainty quantification of the multicomponent system, which we present in Section 4, requires that we deconstruct then reconstruct this multicomponent interface. To mitigate this challenge we exploit the fact that many of the AEDT input variables have an insignificant

Table 4

Presented here are the fuel consumption results over the three flight trajectories. The TASOpt row represents an aircraft generated by and flown in TASOpt. The AEDT row represents the TASOpt aircraft imported into the AEDT component through the multicomponent coupling procedure and then flown on the same flight trajectory as the TASOpt flight trajectory.

	Flight A (850 [nmi])		Flight B (1520 [nmi])		Flight C (2300 [nmi])	
	Fuel [lb]	% Rel Error	Fuel [lb]	% Rel Error	Fuel [lb]	% Rel Error
TASOpt	5015.6	-	8715.3	-	13186.4	-
AEDT	5284.7	5.37	9737.4	9.62	13594.4	3.09

impact on the uncertainty in the system output of interest. This permits us to reduce the dimensions of the multicomponent interface to only those AEDT input variables that have a significant influence on the system output of interest uncertainty. As a result, we perform the decomposition-based uncertainty quantification on a reduced multicomponent interface. In this section, we quantify the influence of the AEDT input variables on the system output of interest and use this information to determine which of the AEDT input variables should take part in the decomposition-based uncertainty quantification.

We quantify the influence of the AEDT input variables on the system output of interest using a variance-based global sensitivity analysis of AEDT [27]. A variance-based global sensitivity analysis of AEDT apportions the output of interest variance amongst the AEDT input variables. Implicit in a variance-based global sensitivity analysis is the assumption that the variance characterizes the uncertainty of the output of interest [9, 8]. However, in many applications the variance only provides a restricted representation of the output of interest uncertainty. In this work, we will assume the variance adequately characterizes the output of interest uncertainty for our purposes, however, in general the results of a variance-based global sensitivity analysis should be carefully interpreted. In addition, since the inputs to AEDT are obtained from the outputs of TASOpt, there is no guarantee that the AEDT inputs are independently distributed, which is a strong assumption in many methods for performing variance-based global sensitivity analysis [27]. As a result, we implement a generalized analysis of variance (ANOVA) dimensional decomposition which addresses dependent variables explicitly, that is, without invoking any isoprobabilistic transformations [24].

A generalized ANOVA dimensional decomposition aims to represents the high-fidelity AEDT component using multivariate orthonormal polynomials as basis functions. The multivariate orthonormal polynomials are constructed with respect to the AEDT dependent input probability distribution. The multivariate orthonormal polynomials form the basis for the high-dimensional model representation (HDMR) subcomponent functions by which the coefficients are solved through a coupled system of equations satisfying the hierarchical orthogonal condition of the subcomponent functions. The AEDT component, which we represent here as f, admits a unique, finite, hierarchical expansion,

$$
\begin{aligned}
f(\mathbf{t}) &= f_{\{0\}} + \sum_{i=1}^{d} f_{\{i\}}(t_i) + \sum_{i=1}^{d} \sum_{j>i}^{d} f_{\{i,j\}}(t_i, t_j) + \cdots + f_{\{1,2,\ldots,d\}}(\mathbf{t}), \\
&= \sum_{\mathcal{A} \subseteq \{1,\ldots,d\}} f_{\mathcal{A}}(\mathbf{t}_{\mathcal{A}}),
\end{aligned}
$$

(3.2)

where $\mathbf{t} = [t_1, t_2, \ldots, t_d]^\top$ are the inputs to f, $f_{\{0\}}$ is a constant, $f_{\{i\}}$ is a function of only t_i, $f_{\{i,j\}}$ is a function of only t_i and t_j, etc. [24]. Using the generalized ANOVA dimensional decomposition, the expectation of the AEDT output of interest (i.e., $PFEI$) is given by the first subcomponent function (i.e., $\mathcal{A} = \{0\}$),

$$(3.3) \qquad\qquad \mu = \mathbb{E}_X[f(\mathbf{t})] = f_{\{0\}},$$

where $X : \Omega \to \mathbb{R}^d$ defined on the probability space $(\Omega, \mathcal{F}, \mathbb{P})$ is the AEDT random input variable. Additionally, the variance of the AEDT output of interest is given by

$$(3.4) \quad \sigma^2 = \mathbb{E}_X[(f(\mathbf{t}) - \mu)^2] = \sum_{0 \neq \mathcal{A} \subseteq \{1,\ldots,d\}} \mathbb{E}_X[f_{\mathcal{A}}^2(\mathbf{t}_{\mathcal{A}})] + \sum_{\substack{0 \neq \mathcal{A}, \bar{\mathcal{A}} \subseteq \{1,\ldots,d\} \\ \mathcal{A} \not\subseteq \bar{\mathcal{A}} \not\subseteq \mathcal{A}}} \mathbb{E}_X[f_{\mathcal{A}}(\mathbf{t}_{\mathcal{A}})f_{\bar{\mathcal{A}}}(\mathbf{t}_{\bar{\mathcal{A}}})],$$

where $d = 100$. The second sum accounts for the covariance contributions from two distinct (i.e., $\mathcal{A} \subseteq \{1,\ldots,d\}$ and $\bar{\mathcal{A}} \subseteq \{1,\ldots,d\}$) non-constant component functions that are not hierarchically orthogonal.

When the input variables involve dependent probability distributions, we require a triplet of global sensitivity indices [24]. The three $\mathcal{A}$-variate global sensitivity indices of $f_{\mathcal{A}}$, where $\mathcal{A} \subseteq \{1,\ldots,d\}$, are denoted by $S_{\mathcal{A},v}$, $S_{\mathcal{A},c}$, and $S_{\mathcal{A}}$, and are defined by the ratios

$$(3.5) \qquad\qquad S_{\mathcal{A},v} = \frac{\mathbb{E}_X[f_{\mathcal{A}}^2(\mathbf{t}_{\mathcal{A}})]}{\sigma^2},$$

$$(3.6) \qquad\qquad S_{\mathcal{A},c} = \frac{\sum_{\substack{0 \neq \bar{\mathcal{A}} \subseteq \{1,\ldots,d\} \\ \mathcal{A} \not\subseteq \bar{\mathcal{A}} \not\subseteq \mathcal{A}}} \mathbb{E}_X[f_{\mathcal{A}}(\mathbf{t}_{\mathcal{A}})f_{\bar{\mathcal{A}}}\mathbf{t}_{\bar{\mathcal{A}}})]}{\sigma^2},$$

$$(3.7) \qquad\qquad S_{\mathcal{A}} = S_{\mathcal{A},v} + S_{\mathcal{A},c}.$$

The first two indices, $S_{\mathcal{A},v}$ and $S_{\mathcal{A},c}$, represent the normalized versions of the variance contribution from $f_{\mathcal{A}}$ to σ^2 and of the covariance contributions from $f_{\mathcal{A}}$ and all $f_{\bar{\mathcal{A}}}$, such that $\mathcal{A} \not\subseteq \bar{\mathcal{A}} \not\subseteq \mathcal{A}$, to σ^2. They are termed the variance-driven global sensitivity index and the covariance-driven global sensitivity index, respectively, of $f_{\mathcal{A}}$. The third index, $S_{\mathcal{A}}$, referred to as the total global sensitivity index of $f_{\mathcal{A}}$, is the sum of variance and covariance contributions to σ^2 that are associated with $f_{\mathcal{A}}$. Summing over all of the triplet global sensitivity indices adds up to

$$(3.8) \qquad \sum_{0 \neq \mathcal{A} \subseteq \{1,\ldots,d\}} S_{\mathcal{A},v} + \sum_{0 \neq \mathcal{A} \subseteq \{1,\ldots,d\}} S_{\mathcal{A},c} = \sum_{0 \neq \mathcal{A} \subseteq \{1,\ldots,d\}} S_{\mathcal{A}} = 1.$$

We use these sensitivity indices to identify the most influential AEDT input variables on the AEDT output of interest. We construct the generalized ANOVA dimensional decomposition of the AEDT component using first-order basis functions (i.e., $\mathcal{A} = \{i\}$) with at most

first-degree polynomials as the subcomponent functions. The AEDT random input variable is distributed according to a multivariate Gaussian distribution where the mean and covariance terms are computed using a subset of TASOpt output realizations. The reason for using TASOpt output realizations is because we did not have adequate experience or prior knowledge of this system to accurately guess these parameters; instead, a few TASOpt realization provide an informed estimate. With the subcomponent functions in hand, we compute the absolute maximum allowable variation (i.e., $|S_{\mathcal{A},v}| + |S_{\mathcal{A},c}|$) due to each AEDT random input variable. Using this criterion we rank the AEDT random input variables in decreasing order of influence on the AEDT output of interest, as illustrated in Figure 4. These results confirm that only a small subset, here just 15 AEDT random input variables, of the original d AEDT random input variables have a substantial influence on the AEDT output of interest variation.
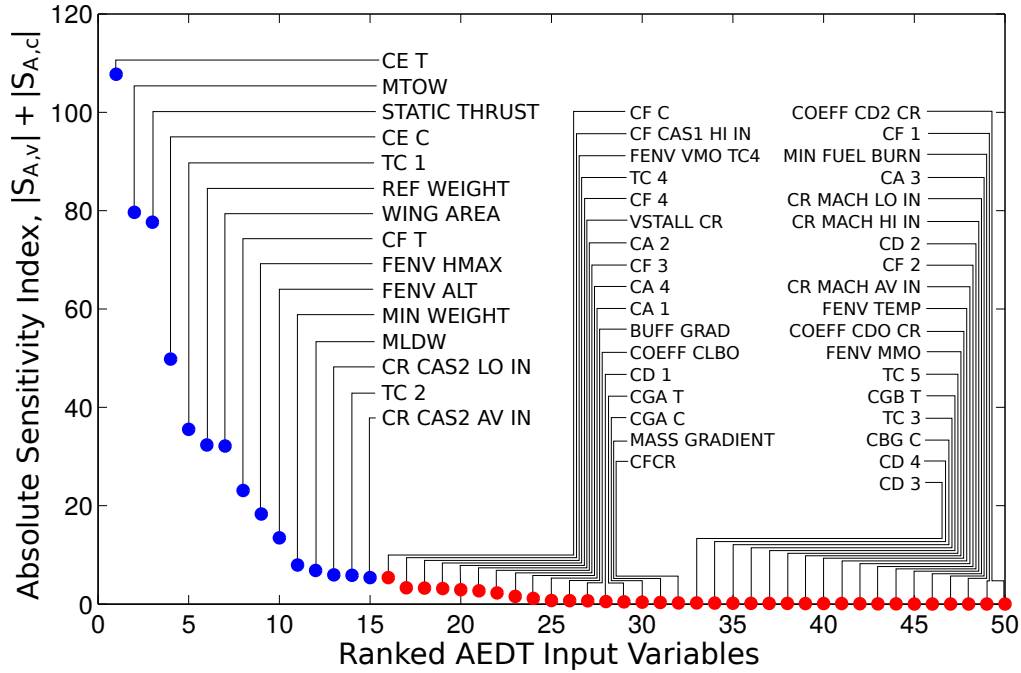
Figure 4. *This plot presents the absolute variance- and covariance-driven sensitivity indices from each of the AEDT random input variables on the AEDT fuel consumption performance variance. This plot illustrates that the absolute variance- and covariance-driven sensitivity indices decay rapidly and that 15 AEDT random input variables capture almost all of the AEDT fuel consumption performance variance.*

At this stage in the analysis we could approximately identify which of the TASOpt inputs contribute the most to the variation of the important variables presented in Figure 4 by performing a global sensitivity analysis of TASOpt with respect to the 15 important variables. However, since our system is only composed of two components, there is no need to do this— we can complete the uncertainty quantification study as is, through the computationally efficient procedure described in the next section. If our system were composed of more than two components, then one could possibly justify performing global sensitivity analysis on more than one component to reduce the coupling interface dimensions across two or more components.

4. Uncertainty Quantification. Applying the results from Section 3, we reduce the multicomponent coupling interface and decompose the multicomponent system as illustrated in Figure 5. Consequently, instead of performing the uncertainty quantification of the multicomponent system presented in Figure 1, we perform a decomposition-based uncertainty quantification of the reduced multicomponent system presented in Figure 5.
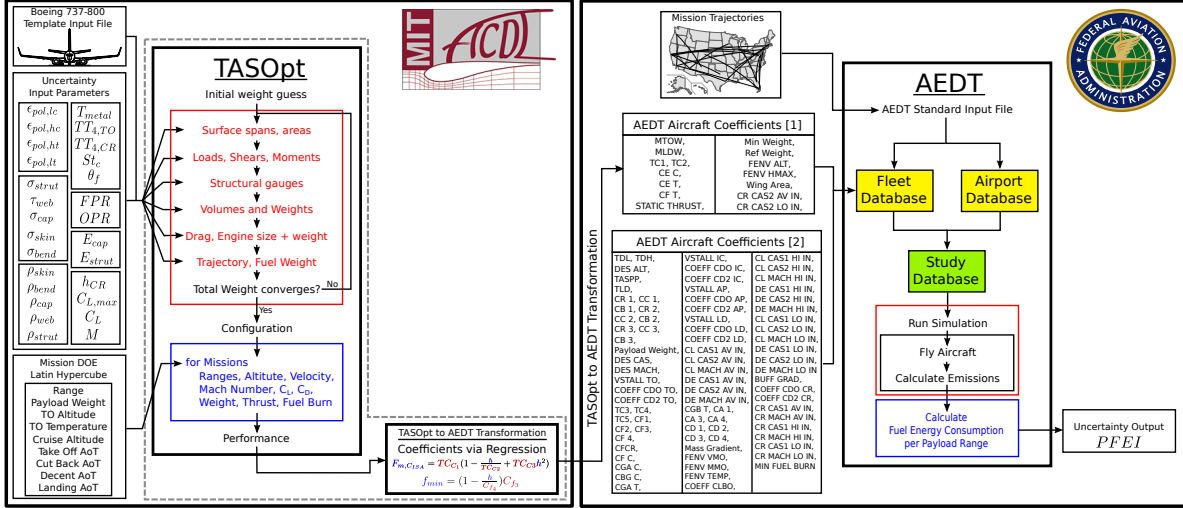

Figure 5. *We partitioned the AEDT input variables into two sets; an influential set and a noninfluential set. The noninfluential set contains AEDT input variables which were deemed not to influence, by the AEDT component global sensitivity analysis, the AEDT output of interest. The influential set contains AEDT random input variables which were labeled as influential by the AEDT component global sensitivity analysis.*

4.1. Uncertainty Analysis. As illustrated on the left in Figure 6, we wish to perform the multicomponent system uncertainty analysis that propagates uncertainty in system inputs to uncertainty in system outputs. To tackle the complexity of a multicomponent uncertainty analysis we propose to decompose the system uncertainty analysis into individual component-level uncertainty analyses that are then assembled into the desired multicomponent system uncertainty analysis [3]. The decomposed system uncertainty analysis is illustrated on the right in Figure 6. The decomposition-based uncertainty analysis approach comprises of two main procedures which are illustrated in Figure 7: (1) local uncertainty analysis: perform a local Monte Carlo uncertainty analysis on each component using their respective proposal distributions; and (2) global compatibility satisfaction: resolve the coupling among the components without any further evaluations of the components or of the system as a whole.

In the offline phase, demonstrated on the top in Figure 7, each local uncertainty analysis is performed concurrently for each component. The challenge created by decomposition is that the distribution functions of the inputs for each component are unknown when conducting the local uncertainty analysis. Therefore, we propose an initial distribution function for each component input, which we refer to as the *proposal distribution function*. Local uncertainty analysis uses the proposal distribution function to generate samples of the uncertain component inputs and propagate them through the component analysis to generate corresponding samples of component outputs.
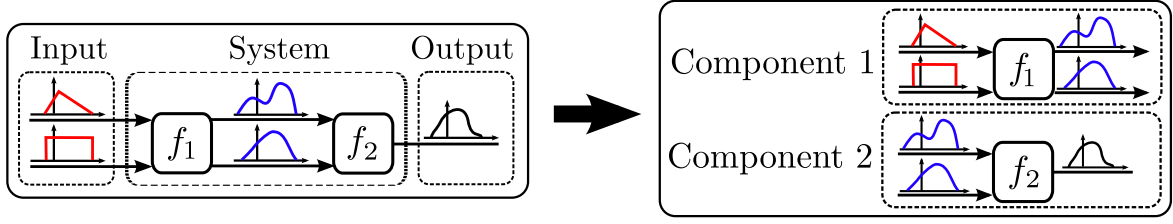
Figure 6. *The proposed method of multicomponent uncertainty analysis decomposes the problem into manageable components, similar to decomposition-based approaches used in multidisciplinary analysis and optimization, and synthesizes the system uncertainty analysis without needing to evaluate the system in its entirety.*
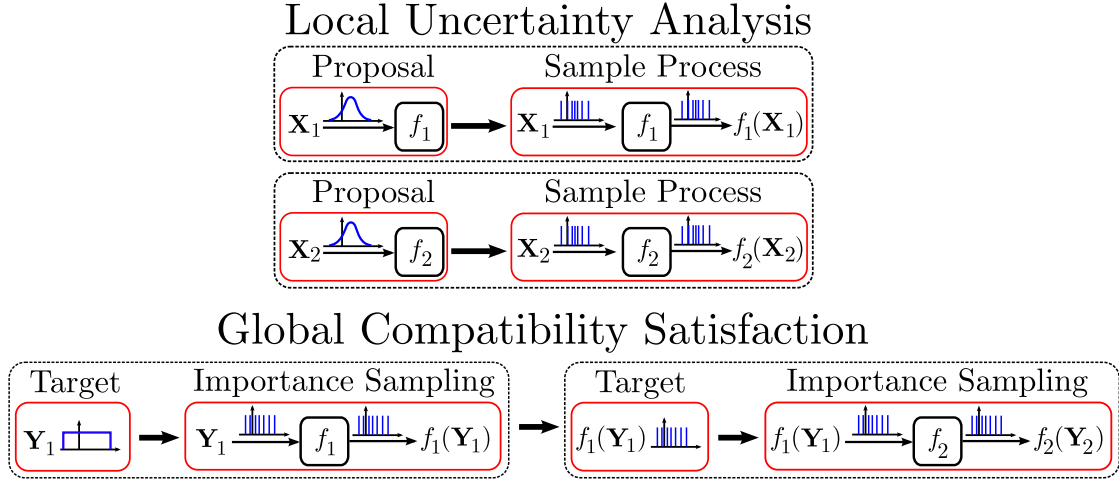

Figure 7. *The process depicts the local uncertainty analysis and global compatibility satisfaction for our two component system. First, local uncertainty analysis is performed on each component. Second, global compatibility satisfaction uses importance sampling to update the proposal samples so as to approximate the target distribution. Here we use X and Y to represent the proposal and target random variables, respectively.*

In the online phase, demonstrated on the bottom in Figure 7, we learn the true distribution function of the inputs of each component. We refer to these true distribution functions as the *target distribution functions.* For those component inputs that correspond to system inputs, the target distribution functions represent the particular specified scenario under which we wish to perform the system uncertainty analysis. For those component inputs that correspond to coupling variables (i.e., they are outputs from upstream components), the target distribution functions are specified by the uncertainty analysis results of the corresponding upstream component(s).

Global compatibility satisfaction is ensured by starting with the most upstream components of the system and approximating their respective target distribution functions using importance sampling on the corresponding proposal distribution functions. The approach we implement for the importance sampling step entirely avoids the probability density function and works with the well-defined and determinable empirical distribution function associated with the random samples [4]. A key attribute of the approach is its scalability: it lends it-

self well to handling a large number of samples through a scalable optimization algorithm. The approach also scales to problems with high-dimensional distributions, an important property we use in this engineering example. The updated output importance weighted samples of the upstream component then define the target distribution function for the downstream component. The process of importance sampling is repeated for the downstream component resulting in the downstream components importance weighted output samples. The downstream components importance weighted output samples characterizes the multicomponent systems outputs of interest uncertainty under the target distribution and is used to quantify the desired statistics of interest.

The proposal distribution selected for the AEDT component is the same distribution used to construct the generalized ANOVA dimensional decomposition in Section 3 with the covariance term multiplied by a factor of three. The proposal covariance term was multiplied by a factor of three to ensure the unknown target distribution from the upstream TASOpt component is supported by the AEDT input proposal distribution. In the situation that the input proposal distribution does not support the forthcoming target distribution we must resample the AEDT module using the latest information from the forthcoming target distribution. The uncertainty analysis results are presented in Figure 8. The results illustrate the system output of interest distribution function under three different scenarios. The first scenario is the outcome of running the AEDT component under the proposal distribution assumption. The second scenario is produced by performing an all-at-once uncertainty analysis of the system illustrated in Figure 1 using Monte Carlo simulation. The last scenario is the result of performing a decomposition-based uncertainty analysis of the system illustrated in Figure 5.
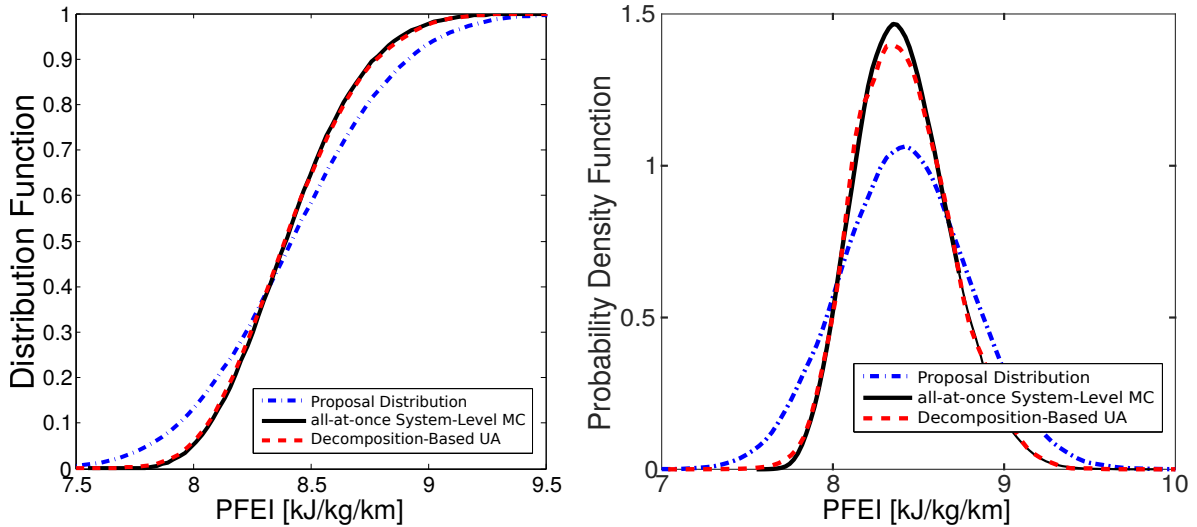

Figure 8. *The AEDT fuel consumption performance distribution is shown, on the left, using the AEDT output proposal distribution, all-at-once Monte Carlo uncertainty analysis, and the decomposition-based uncertainty analysis. On the right are the resulting probability density functions. These results suggest that our decomposition-based uncertainty analysis performed adequately which implies the change of measure across the 15 AEDT random input variables was successful and that the correct 15 AEDT random input variables were selected by the AEDT component-level global sensitivity analysis.*

These results demonstrate that our decomposition-based uncertainty analysis of the reduced system in Figure 5 accurately produces the result from the standard approach, the all-at-once Monte Carlo simulation of the full system in Figure 1. The discrepancy between the decomposition-based approach and the all-at-once Monte Carlo simulation can be attributed to performing the importance sampling on a subset of the coupling variables using only a finite number of samples. The results presented imply that we successfully identified the 15 influential AEDT random input variables and also that we accurately performed the importance sampling procedure across the resulting 15-dimensional interface between the TASOpt component and the AEDT component. By reducing the dimensions of the multicomponent interface, we illustrated that our decomposition-based uncertainty analysis approach can be extended to calculate the relevant statistics and failure probabilities of complex and high-dimensional systems.

4.2. Global Sensitivity Analysis. The purpose of a global sensitivity analysis is to identify how the variability in a system output quantity of interest is related to a system input and which of the system input sources dominate the response of the system output. Our motivation for a system-level global sensitivity analysis is research prioritization: which system input factor is the most deserving of further analysis or measurement? To address our objective we apply the Sobol' variance-based global sensitivity analysis method, which quantifies the amount of variance that each input factor contributes to the unconditional variance of the output [28].

To perform the global sensitivity analysis of the multicomponent system we apply the generalized ANOVA framework presented in Section 3 to this context, where f now represents the entire multicomponent system. Since the multicomponent system inputs are independently distributed we can discard the covariance contribution in Equation 3.8 from our $\mathcal{A}$-variate global sensitivity indices. The resulting global sensitivity indices of the multicomponent system,

$$(4.1) \qquad 1 = \sum_{i=1}^{d} S_{\{i\},v} + \sum_{i<j}^{d} S_{\{i,j\},v} + \cdots + S_{\{1,2,\ldots,d\},v},$$

apportion the output variance amongst the system inputs. Global sensitivity indices with only a single subscript (e.g., $S_{\{i\}}$) are called main effect indices. Inputs with large main effect indices are known as the "most influential factors", or the inputs that, on average, once fixed, would result in the greatest reduction in variance. Global sensitivity indices with multiple subscripts (e.g., $S_{\{i,j\}}$) are called interaction effect indices.

In this context, we cannot construct a generalized ANOVA dimensional decomposition of the multicomponent system since this would result in having to evaluate the entire multicomponent system. Instead, to evaluate the global sensitivity indices using a decomposition-based approach, we first use a restated but equivalent definition of the global sensitivity indices. For example, the main effect indices can be restated using the conditional and unconditional variances,

$$(4.2) \qquad S_i = \frac{var_{X_i}(\mathbb{E}_{X_i^c}[f_{\{i\}}])}{\sigma^2},$$

where X_i is the ith component of the vector of random variables X and X_i^c is the vector containing all components of X except X_i [28].

Since Equation 4.2 requires evaluating the expectation of f conditioned on random variables, we cannot yet directly apply a decomposition-based methodology in a straightforward way. Instead, we will approximate Equation 4.2 by evaluating the expectation of f conditioned on the random variable existing in a finite range. By relaxing the conditional dependence in this way, we can evaluate the expectations contained within Equation 4.2 using our decomposition-based uncertainty analysis algorithm, since expectation is just a statistic of interest. To construct these conditional sets of finite range, we partition the input space into a finite number of bins [28]. For each bin we evaluate the expectation contained in Equation 4.2 using our decomposition-based uncertainty analysis algorithm and modifying the system input target distribution to be contained in the bin of interest. After evaluating the expectations over each bin, we can evaluate the variance over those expectations to approximate Equation 4.2. This procedure relies only on the offline step of our decomposition-based uncertainty analysis algorithm. Therefore we can repeat these steps for each system input without having to evalute the components comprising the system.

The results of the system-level main sensitivity indices are presented in Figure 9. The results depict the system-level main sensitivity indices computed using the all-at-once Monte Carlo simulation approach of the system illustrated in Figure 1 and the decomposition-based approach of the system illustrated in Figure 5. These results confirm that our decomposition-based sensitivity analysis algorithm can accurately quantify the main sensitivity indices of the system in Figure 1. As previously mentioned, the decomposition-based sensitivity analysis algorithm hinges on the fact that we can evaluate the decomposition-based uncertainty analysis. The main sensitivity indices suggest that the output of interest variation is mostly dominated by a handful of aircraft technological and operational variables. That is, by improving our understanding of these TASOpt random input variables through research, we can reduce the variation of the overall system output of interest, which is beneficial for decision- and policy-making.

5. Conclusion. This paper presents uncertainty quantification of a realistic application problem involving a complex multicomponent system model of the environmental impacts of aviation technologies and operations. The multicomponent system comprises a conceptual-level aircraft design tool and an environmental impacts tool. The challenges of applying uncertainty quantification to this multicomponent system include long computational run times, a high-dimensional component-to-component interface, and a lack of software integration among the system components. These challenges are overcome through a combination of dimensionality reduction and decomposition. A component-level global sensitivity analysis identifies the most influential component-to-component interface variables and permits reduction of the dimensionality of the component-to-component interface. With this reduction in dimensions, a decomposition-based uncertainty quantification approach becomes feasible. This permits local uncertainty analyses to be conducted, and the results synthesized to compute system-level uncertainty estimates and system-level sensitivity indices. The results reveal the most important sources of uncertainty across the system, which informs policy decision-making as well as future tool development. Future work will extend these ideas to different and more
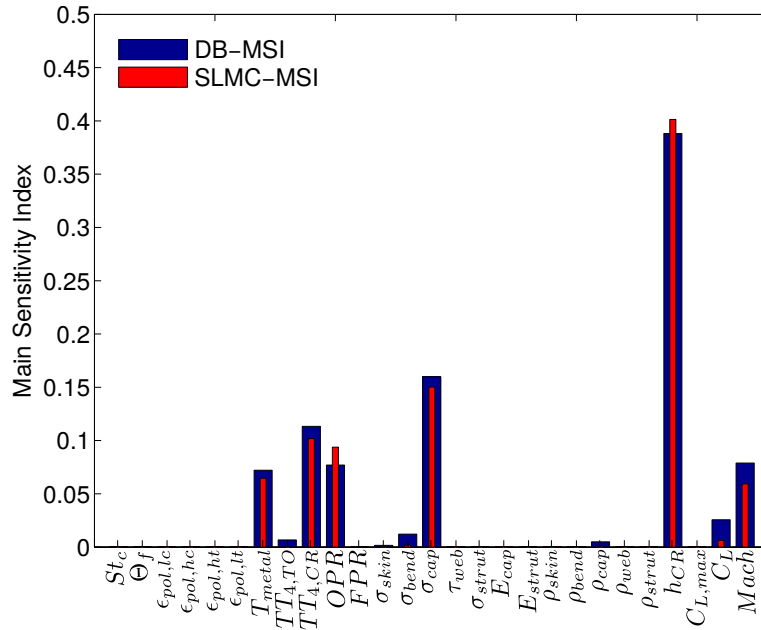
Figure 9. *The system-level main sensitivity indices are shown here using the all-at-once Monte Carlo global sensitivity analysis and our proposed decomposition-based global sensitivity analysis. These results suggest that our decomposition-based global sensitivity analysis performed adequately and that only a handful of technological and operational system input variables have a significant influence, on average, on the system output of interest. A description of the system inputs are provided in Table 1*

complex architectures of feed-forward and feed-back multicomponent systems. This will require accounting for dependency among variables using only the samples but with no explicit description of their underlying probability density functions. An additional future direction includes performing decomposition-based uncertainty quantification with a goal-oriented objective. The aim in this case is to minimize the system complexity while approximating the quantity of interest to within a specified tolerance.

REFERENCES

[1] ICAO 2010a. Report of the committee on aviation environmental protection, eighth meeting. Technical Report CAEP/8-IP/30, Montreal, Canada, February 2010.

[2] ICAO 2010b. 37th session of the ICAO assembly, resolution A37-19: Consolidated statement of continuing ICAO policies and practices related to environmental protection climate change. Technical report, Montreal, Canada, November 2010.

[3] Sergio Amaral, Douglas Allaire, and Karen Willcox. A decomposition-based approach to uncertainty analysis of feed-forward multicomponent systems. *International Journal for Numerical Methods in Engineering*, 100(13):982–1005, 2014.

[4] Sergio Amaral, Douglas Allaire, and Karen Willcox. Optimal l_2-norm empirical importance weights for the change of probability measure. *Statistics and Computing Journal*, 100(13):982–1005, 2016.

[5] Maarten Arnst, Roger Ghanem, Eric Phipps, and John Red-Horse. Dimension reduction in stochastic modeling of coupled problems. *International Journal for Numerical Methods in Engineering*, 92(11):940–968, 2012.

[6] Maarten Arnst, Roger Ghanem, Eric Phipps, and John Red-Horse. Measure transformation and efficient quadrature in reduced-dimensional stochastic modeling of coupled problems. *International Journal for Numerical Methods in Engineering*, 92(12):1044–1080, 2012.

[7] Maarten Arnst, Roger Ghanem, Eric Phipps, and John Red-Horse. Reduced chaos expansions with random coefficients in reduced-dimensional stochastic modeling of coupled problems. *International Journal for Numerical Methods in Engineering*, 97(5):352–376, 2014.

[8] Emanuele Borgonovo. A new uncertainty importance measure. *Reliability Engineering & System Safety*, 92(6):771–784, 2007.

[9] Emanuele Borgonovo, William Castaings, and Stefano Tarantola. Moment independent importance measures: New results and analytical test cases. *Risk Analysis*, 31(3):404–428, 2011.

[10] Robert Braun and Ilan Kroo. Development and application of the collaborative optimization architecture in a multidisciplinary. *In: Alexandrov, N., Hussaini, M.Y. (eds.) Multidisciplinary design optimization: state of the art. SIAM Journal of Optimization*, 80:98–116, 1997.

[11] Anirban Chaudhuri and Karen Willcox. Multifidelity uncertainty propagation in coupled multidisciplinary systems. In *18th AIAA Non-Deterministic Approaches Conference, San Diego, CA*, 2016.

[12] The Boeing Company. Boeing: Airport compatibility - CAD 3-view drawings for airport planning purposes. Boeing.com [Online; posted 15-May-2015].

[13] Paul Constantine, Eric Phipps, and Timothy Wildey. Efficient uncertainty propagation for network multiphysics systems. *International Journal for Numerical Methods in Engineering*, 2014.

[14] Nick Cumpsty, Juan Alonso, Serge Eury, Lourdes Maurice, Bengt-Olov Nas, Malcolm Ralph, and Robert Sawyer. Report of the independent experts on fuel burn reduction technology goals. In *International Civil Aviation Organization (ICAO), Committee on Aviation Environmental Protection (CAEP), Steering Group Meeting*, 2010.

[15] Mark Drela. Simultaneous optimization of the airframe, powerplant, and operation of transport aircraft. *Hamilton Place, London*, 2010.

[16] Hyung Min Kim, Nestor Michelena, Panos Papalambros, and Tao Jiang. Target cascading in optimal system design. *Journal of Mechanical Design*, 125(3):474–480, 2003.

[17] Jonathan Koopmann and Meghan Ahearn. Aviation environmental design tool (aedt) 2a: Technical manual. Technical report, 2012.

[18] Ilan Kroo. Distributed multidisciplinary design and collaborative optimization. In *VKI lecture series on Optimization Methods & Tools for Multicriteria/Multidisciplinary Design*, number November 15–19, pages 1–22, 2004.

[19] David Lee, David Fahey, Piers Forster, Peter Newton, Ron Wit, Ling Lim, Bethan Owen, and Robert Sausen. Aviation and global climate change in the 21st century. *Atmospheric Environment*, 43(22):3520–3537, 2009.

[20] Yu Liu, Xiaolei Yin, Paul Arendt, Wei Chen, and Hong-Zhong Huang. A hierarchical statistical sensitivity analysis method for multilevel systems with shared variables. *Journal of Mechanical Design*, 132(3):031006, 2010.

[21] Jay Martin and Timothy Simpson. A methodology to manage system-level uncertainty during conceptual design. *Journal of Mechanical Design*, 128(4):959–968, 2006.

[22] George Noel, Doug Allaire, Stuart Jacobson, Karen Willcox, and Rebecca Cointin. Assessment of the aviation environmental design tool. In *Proceedings of the Eighth USA/Europe Air Traffic Management Research and Development Seminar (ATM2009), Napa, CA, June*, volume 29, 2009.

[23] A Nuic. User manual for the base of aircraft data (bada) revision 3.10. *Atmosphere*, 2010:001, 2010.

[24] Sharif Rahman. A generalized ANOVA dimensional decomposition for dependent probability measures. *SIAM/ASA Journal on Uncertainty Quantification*, 2(1):670–697, 2014.

[25] Christopher Roof, Andrew Hansen, Gregg Fleming, Ted Thrasher, Alex Nguyen, Cliff Hall, F Grandi, B Kim, S Usdrowski, and P Hollingsworth. Aviation environmental design tool (AEDT) system architecture. *Doc# AEDT-AD-01*, 2007.

[26] Daniel Rutherford and Mazyar Zeinali. Efficiency trends for new commercial jet aircraft 1960 to 2008. *International Council on Clean Transportation*.

[27] Andrea Saltelli. Global sensitivity analysis: An introduction. In *Proc. 4th International Conference on Sensitivity Analysis of Model Output (SAMO04)*, pages 27–43, 2004.

[28] Andrea Saltelli, Marco Ratto, Terry Andres, Francesca Campolongo, Jessica Cariboni, Debora Gatelli, Michaela Saisana, and Stefano Tarantola. *Global sensitivity analysis: the primer*. John Wiley & Sons, 2008.

[29] Shankar Sankararaman and Sankaran Mahadevan. Likelihood-based approach to multidisciplinary analysis under uncertainty. *Journal of Mechanical Design*, 134(3):031008, 1–12, 2012.

[30] Ralph Smith. *Uncertainty quantification: theory, implementation, and applications*, volume 12. SIAM, 2013.

[31] Jaroslaw Sobieszczanski-Sobieski, Jeremy Agte, and Robert Sandusky. Bilevel integrated system synthesis. *AIAA Journal*, 38(1):164–172, 2000.

[32] Wen Yao, Xiaoqian Chen, Wencai Luo, Michel van Tooren, and Jian Guo. Review of uncertainty-based multidisciplinary design optimization methods for aerospace vehicles. *Progress in Aerospace Sciences*, 47(6):450–479, 2011.

[33] Xiaolei Yin and Wei Chen. A hierarchical statistical sensitivity analysis method for complex engineering systems design. *Journal of Mechanical Design*, 130(7):071402, 2008.